Numerical simulation of tridimensional electromagnetic shaping of liquid metals

Michel Pierre and Jean R. Roche

Université de Nancy I, Département de Mathématiques,
URA CNRS 750, Projet NUMATH INRIA-lorraine
BP 239, F-54506 Vandoeuvre les Nancy Cédex, France

Summary. We describe a numerical method to compute free surfaces in electromagnetic shaping and levitation of liquid metals. We use an energetic variational formulation and optimization techniques to compute a critical point. The surfaces are represented by piecewise linear finite elements. Each step of the algorithm requires solving an elliptic boundary value problem in the exterior of the intermediate surfaces. This is done by using an integral representation on these surfaces.

Mathematics Subject Classification (1991): 65N30, 65K10, 65N38, 65R30

1. Introduction

Our goal is to develop numerical method to compute free surfaces in electromagnetic shaping and levitation of liquid metals. We introduce quasi-Newton optimization techniques in an energetic variational formulation framework.

In the two-dimensional case a numerical simulation has been developed [2, 4, 5, 10, 16, 17, 20, 25]. The physical model concerns the case of a vertical column of liquid metal falling down in an electromagnetic field created by vertical conductors.

The same model in the tridimensional case represents a bubble of liquid metal levitating in an electromagnetic field. We want to compute the shape of the bubble [3, 11–14]. We assume the frequency of the imposed current is very high so that the magnetic field does not penetrate into the metal and the electromagnetic forces are reduced to the magnetic pressure acting on the interface.

We denote by ω the exterior in $\mathbf{R}^3$ of the domain filled by the liquid metal and by Γ its boundary (here a surface).

Correspondence to: M. Pierre

Under above assumptions, the surface Γ is characterized by the following equilibrium equations:

$$(1.1) \qquad \nabla \wedge B = \mu_0 j_0 \quad \text{in } \omega$$

$$(1.2) \qquad \nabla \cdot B = 0 \quad \text{in } \omega$$

$$(1.3) \qquad B \cdot n = 0 \quad \text{on } \Gamma = \partial \omega$$

$$(1.4) \qquad \frac{\|B\|^2}{2\mu_0} + \sigma \vartheta + \rho g z = P \quad \text{on } \Gamma$$

where j_0 is the current density, B the magnetic field, μ_0 the magnetic permeability, ρ the density of the charge, g the gravitational acceleration, z the height, $\mathscr{C}$ the mean curvature of Γ, σ the surface tension and n the unit normal vector directed towards ω. The constant P is an unknown of the problem. We denote by $\Omega = {}^c\omega$ the complement of ω.

The total energy of the system is given by [3, 9, 26, 28]

$$(1.5) \qquad E(\Omega) = \frac{-1}{2\mu_0} \int_\omega \|B\|^2 \, dx + \sigma \int_\Gamma d\gamma + \int_\Omega \rho g z \, dx$$

where B is solution of (1.1)–(1.3). With some usual hypotheses, a critical point of $E(\Omega)$ under the constraint that meas (Ω) be given, satisfies the nonlinear equilibrium relation (1.4) which characterizes the boundary Γ.

A quasi-Newton optimization method is used here to compute a critical point of the total energy $\Omega \to E(\Omega)$. This means that one must compute the gradient of E with respect to Ω at each iteration. The main part of the gradient computation is solving the exterior problem (1.1)–(1.3) for each intermediate domain Ω_k. For this we introduce a boundary integral representation on the surface $\Gamma_k = \partial \Omega_k$. This is quite convenient here since the computation of the gradient of E requires only the values of the magnetic field on the surface Γ_k. The computation is done by using a piecewise linear approximation of Ω. The energy (1.5) is replaced by a corresponding discretized energy. Details are given in Sect. 4. The derivatives with respect to Ω of the various terms in $E(\Omega)$ are recalled in Sect. 3.

2. Computing the magnetic field B

Let us consider the problem (1.1)–(1.3). Let ω be an open subset of $\mathbb{R}^3$. We set [6, 23]

$$(2.1) \qquad W^1(\omega) \text{ the closure of } D(\bar{\omega}) \text{ for the semi-norm}$$

$$\varphi \to \|\nabla \varphi\|_{L^2}(\omega)$$

$$W^2(\omega) \text{ the closure of } D(\bar{\omega}) \text{ for the semi-norm}$$

$$\varphi \to \sum_{i,j} \left\| \frac{\partial^2 \varphi}{\partial x_i \partial x_j} \right\|_{L^2}(\omega)$$

Throughout this paper, we assume that:

(2.2) $\bar{\omega}$ = complement of an open set Ω with boundary $\Gamma = \partial\Omega = \partial\omega$
of class C^2 and ω is simply connected

Then it is well known that $\varphi \to \|\nabla\varphi\|_{L^2(\omega)}$ is a norm in $W^1(\omega)$ [6]. We also introduce:

(2.3) $j_0 \in (L^2(\mathbb{R}^3))^3$ with compact support and $\nabla \cdot j_0 = 0$ in $\mathscr{D}'(\mathbb{R}^3)$.

Lemma 2.1. *There exists a unique solution B of the following differential system:*

$$
\begin{array}{lll}
\text{(2.4.a)} & B \in W^1(\omega)^3 & \\
\text{(2.4.b)} & \nabla \wedge B = \mu_0 j_0 & \text{in } \omega \\
\text{(2.4.c)} & \nabla \cdot B = 0 & \text{in } \omega \\
\text{(2.4.d)} & B \cdot n = 0 & \text{on } \Gamma
\end{array}
$$

(2.4)

Moreover, if we set:

(2.5)
$$
B_1(x) = \frac{\mu_0}{4\pi} \int_{\mathbb{R}^3} \frac{j_0(y) \wedge (x - y)}{\|x - y\|^3}\, dy
$$

then

(2.6) $\nabla \wedge B_1 = \mu_0 j_0, \qquad \nabla \cdot B_1 = 0 \qquad in\ \mathbb{R}^3$

(2.7) $B = B_1 + \nabla\varphi \qquad in\ \omega$

where φ is the unique solution of:

$$
\begin{array}{lll}
\text{(2.8.a)} & \varphi \in W^2(\omega) & \\
\text{(2.8.b)} & -\Delta\varphi = 0 & \text{in } \omega \\
\text{(2.8.c)} & \dfrac{\partial\varphi}{\partial n} = -B_1 \cdot n & \text{on } \Gamma.
\end{array}
$$

(2.8)

Proof. Let B_1 be defined by (2.5). Since

$$
\nabla_x\left(\frac{1}{\|x - y\|}\right) = -\frac{(x - y)}{\|x - y\|^3} \quad \text{and} \quad \nabla_y \cdot j_0(y) = 0,
$$

we have by differentiating (2.5)

(2.9) $\nabla \wedge B_1(x) = \dfrac{\mu_0}{4\pi} \int_{\mathbb{R}^3} -\nabla_x \cdot \left(\nabla_x \dfrac{1}{\|x - y\|}\right) \cdot j_0(y)\, dy = \mu_0 j_0(x)$

(2.10) $\nabla \cdot B_1(x) = 0.$

If $\hat{B}_1(\xi)$ denotes the Fourier transform of B_1 in $\mathbb{R}^3$, as $\nabla \wedge B_1$ and $\nabla \cdot B_1$ belong to $L^2(\mathbb{R}^3)$, we have:

(2.11) $\xi \wedge \hat{B}_1(\xi) \in L^2 \quad \text{and} \quad \xi \cdot \hat{B}_1(\xi) \in L^2.$

But:

(2.12)
$$\|\xi \wedge \hat{B}_1(\xi)\|^2 + (\xi \cdot \hat{B}_1(\xi))^2 = \|\xi\|^2 \|\hat{B}_1(\xi)\|^2.$$

Thus $\nabla \cdot B_1$ belongs to L^2 which means:

(2.13)
$$B_1 \in (W^1(\mathbb{R}^3))^3.$$

If we set $B_2 = B - B_1$, (2.9), (2.10), (2.13) imply that problem (2.4) is equivalent to:

(2.14.a) $\qquad B_2 \in (W^1(\omega))^3$

(2.14.b) $\qquad \nabla \wedge B_2 = 0 \qquad$ in ω

(2.14.c) $\qquad \nabla \cdot B_2 = 0 \qquad$ in ω

(2.14.d) $\qquad B_2 \cdot n = -B_1 \cdot n \qquad$ on Γ.

Since ω is simply connected and $\partial\omega$ regular, we have [6, 23]

(2.15) $\quad (B_2 \in (W^1(\omega))^3, \nabla \wedge B_2 = 0) \Leftrightarrow (B_2 = \nabla\varphi, \varphi \in W^2(\omega)).$

Therefore (2.14) is equivalent to (2.8) where

(2.16)
$$B_1 \cdot n \in H^{1/2}(\Gamma), \qquad \int_\Gamma B_1 \cdot n \, d\gamma = 0.$$

But the problem (2.8) has a unique solution [6]. This solution can be represented by a single layer representation [1, 19].

Lemma 2.2. *The solution of the problem* (2.8) *is given by:*

(2.17)
$$\varphi(x) = \frac{1}{4\pi} \int_\Gamma \frac{q(y)}{\|x - y\|} \, d\gamma(y)$$

where q *is the unique solution on* $H^{1/2}(\Gamma)$ *of:*

(2.18)
$$B_1 \cdot n = \frac{1}{2} q(x) + \frac{1}{4\pi} \int_\Gamma q(y) \frac{n(x) \cdot (x - y)}{\|x - y\|^3} \, d\gamma(y).$$

Remark 2.3. Extension to the case where j_0 is a sum of Dirac masses: If j_0 is a compactly supported distribution on ω rather than a function f belonging to $(L^2(\mathbb{R}^3))^3$, the relation (2.5) defines a distribution over $\mathbb{R}^3$ belonging to $W^1(\omega \backslash \text{Supp } j_0)$.

The problem (2.4), except for (2.4.a), can be solved according to (2.7) and (2.8) with $B_1 \cdot n$ and φ as regular as before. The local regularity of B depends on j_0 but is the same as previously (and then the same as the regularity of B_1) in a neighborhood of $\partial\omega$.

This remark is essential since numerical examples are given for distributions concentrated on wires (i.e. thin sets).

3. Variational formulation of the shape optimization problem

We recall here classical results similar to those in [27, 29–31], [25] for the two-dimensional case. We first introduce some notations.

Let ω be an open subset of $\mathbb{R}^3$ such that $\Omega = {}^c\bar\omega$ and let V be a compactly supported vector field of class C^2 over $\mathbb{R}^3$ that is:

$$(3.1) \qquad V \in C^2(\mathbb{R}^3, \mathbb{R}^3), \qquad V \text{ has compact support in } \mathbb{R}^3.$$

We consider transformations of Ω (or ω) given by:

$$(3.2) \qquad \forall x \in \mathbb{R}^3 \quad T_t(x) = x + tV(x).$$

Then we set $\Omega_t = T_t(\Omega)$, $\omega_t = T_t(\omega)$ and we verify that $\Gamma_t = T_t(\Gamma) = \partial\Omega_t$ for t small enough (since $D_x T_t(x) = I + t\, DV(x)$ and thanks to the local inversion theorem).

Given $\sigma > 0$ and $G(x) \in W^{1,1}_{loc}(\mathbb{R}^3, \mathbb{R})$, with each ω_t (or Ω_t) we associate the energy:

$$(3.3) \qquad E(\omega_t) = E_0(\omega_t) + \sigma P(\Omega_t) + \int_{\Omega_t} G(x)\, dx$$

with

$$(3.4) \qquad E_0(\omega_t) = -\frac{1}{2\mu_0} \int_{\omega_t} \|B_{\omega_t}\|^2\, dx$$

where B_{ω_t} is a solution of the problem (2.4) with ω_t instead of ω and $P(\Omega_t)$ is the perimeter of Ω_t. Recall that the perimeter of an open subset $\mathcal{O}$ of $\mathbb{R}^3$ is defined by:

$$(3.5) \qquad P(\mathcal{O}) = \sup\{\langle \nabla \chi_\mathcal{O}, \varphi \rangle_{\mathcal{D}'(\mathbb{R}^3) \times \mathcal{D}(\mathbb{R}_3)},\ \varphi \in \mathcal{D}(\mathbb{R}^3),\ \|\varphi\|_\infty \leq 1\}$$

with $\chi_\mathcal{O}$ the characteristic function of $\mathcal{O}$ defined by:

$$(3.6) \qquad \chi_\mathcal{O}(x) = \begin{cases} 1 & \text{if } x \in \mathcal{O} \\ 0 & \text{otherwise} \end{cases}$$

and

$$\|\varphi\|_\infty = \sup_{x \in \mathbb{R}^3} \left\{ \sum_{i=1}^N \varphi_i(x)^2 \right\}^{1/2}, \qquad \varphi = (\varphi_1, \ldots, \varphi_N).$$

If $\partial\mathcal{O}$ is regular enough then $P(\mathcal{O})$ is the surface area of $\partial\mathcal{O}$.

Lemma 3.1. *The functions* $t \to E_0(\omega_t)$, $P(\Omega_t)$, $\int_{\Omega_t} G(x)\, dx$ *are differentiable at* 0 *and we have:*

$$(3.7) \qquad \left.\frac{d}{dt}\right|_{t=0} E_0(\omega_t) = \frac{1}{2\mu_0} \int_\Gamma \|B_\infty\|^2 (V \cdot n)\, d\gamma$$

$$(3.8) \qquad \left.\frac{d}{dt}\right|_{t=0} P(\Omega_t) = \int_\Gamma \mathscr{C}(V \cdot n)\, d\gamma$$

where $\mathscr{C}$ is the mean curvature of Γ.

(3.9)
$$\frac{d}{dt}\Big|_{t=0}\int_{\Omega_t} G(x)\,dx = \int_\Gamma G(x)(V\cdot n)\,d\gamma.$$

A sketch of the proof. This kind of computations are classical (see for example [21, 26, 27, 30, 31] and [16] for relevant results concerning regularity of boundaries). We recall here some essential steps.

We start with the following classical formula: if g is a sufficiently regular function from $[0,\varepsilon]\times\omega$ on $\mathbf{R}$:

(3.10)
$$\frac{d}{dt}\Big|_{t=0}\int_{\omega_t} g(t,y)\,dy = \int_\omega \frac{\partial g}{\partial t}(0,y)\,dy - \int_{\partial\Gamma} g(y,0)(V\cdot n)\,d\gamma(y)$$

(here n is always the unit normal directed towards ω). It can be obtained by an elementary change of variable $y=T_t(x)$, namely:

(3.11)
$$\int_{\omega_t} g(t,y)\,dy = \int_\omega g(t,y+tV(y))\det(I+tDV(y))\,dy.$$

Then, by differentiation and integration by parts we obtain:

(3.12)
$$\frac{d}{dt}\Big|_{t=0}\int_{\omega_t} g(t,y)\,dy = \int_\omega \left(\frac{\partial g}{\partial t}(0,y)+\nabla_y g(0,y)\cdot V(y)+g(0,y)\nabla\cdot V(y)\right)dy$$
$$= \int_\omega \frac{\partial g}{\partial t}(0,y)\,dy - \int_\Gamma g(y,0)(V\cdot n)\,d\gamma(y).$$

If we apply (3.12) to $g(t,x)=G(x)$ and Ω_t instead of ω_t we obtain (3.9). Applying (3.12) to $g(t,x)=\|B_{\omega_t}(x)\|^2$, we obtain:

(3.13)
$$\frac{d}{dt}\Big|_{t=0}\int_{\omega_t}\|B_{\omega_t}(x)\|^2\,dx$$
$$= 2\int_\omega B_\omega(x)\frac{\partial}{\partial t}\Big|_{t=0} B_{\omega_t}(x)\,dx - \int_\Gamma \|B_\omega(x)\|^2(V\cdot n)\,d\gamma(y).$$

By (2.7), we have:

(3.14)
$$B_{\omega_t}=B_1+\nabla\varphi(t,\cdot),\ \frac{\partial}{\partial t}\Big|_{t=0} B_{\omega_t}=\nabla_x\varphi_t(0,\cdot).$$

Then
$$\int_\omega B_\omega\frac{\partial}{\partial t}\Big|_{t=0} B_{\omega_t}\,dx = \int_\omega B_\omega\cdot\nabla_x\varphi_t(0,\cdot)\,dx = -\int_\Gamma (B_\omega\cdot n)\,\varphi_t\,d\gamma - \int_\omega \varphi_t\nabla\cdot B_\omega\,dx = 0,$$

the last equality coming from (2.4).

The formula (3.8) is classical [29, 31].

Proposition 3.2. *We denote by* $V(\Omega_t)$ *the volume of* Ω_t. *Under the hypotheses* (2.2), (3.1), *the functions* $t \to E(\omega_t)$, $V(\Omega_t)$ *are differentiable at* $t=0$ *and for every* P *constant we have:*

$$\frac{d}{dt}\bigg|_{t=0} (E(\omega_t) - PV(\Omega_t)) = \int_r \left(\frac{1}{2\mu_0}\|B_\omega\|^2 + \sigma\mathscr{C} + G - P\right)(V \cdot n)\, d\gamma.$$

Then (B_ω, ω) *is a solution of the equilibrium system* (1.1)–(1.4) *if and only if there exists* P *such that for every direction* V *satisfying* (3.1) *we have:*

(3.16)
$$\frac{d}{dt}\bigg|_{t=0} (E(\omega_t) - PV(\Omega_t)) = 0.$$

This immediatly follows from Lemma 3.1 and Proposition 3.2. A consequence is that the solution of (1.1)–(1.4) can be considered as a critical point of the total energy $\omega \to E(\omega)$ under the constraint $V(\Omega) = V_0$ (with some regularity hypothesis).

This property is the heart of our numerical approach.

4. Algorithm and discretization

The algorithm consists in constructing a sequence (Γ^k, B^k, Z^k), $k=1, \ldots, n$ where [18]:

Γ^k is an approximation of the surface Γ at the k-th iteration of the algorithm. It is the union of triangles T_ℓ in $\mathbb{R}^3$, $\ell = 1, \ldots, L$. Each triangle is parametrized by a reference triangle of coordinates ξ and η.

The nodes of the T_ℓ triangles are denoted by $x^{\ell,1}$; $x^{\ell,2}$; $x^{\ell,3}$, so that if $x \in T_\ell$

(4.1)
$$x = x(\xi, \eta) = \sum_{i=1}^{3} x^{\ell,i} N_i(\xi, \eta)$$

(4.2)
$$N_1(\xi, \eta) = 1 - \xi - \eta; \quad N_2(\xi, \eta) = \xi; \quad N_3(\xi, \eta) = \eta.$$

If Γ^k is the boundary of the exterior domain ω_k, then B^k is an approximate solution of:

(4.3)
$$\nabla \wedge B = \mu_0 \cdot j_0 \quad \text{in } \omega^k$$
$$\nabla \cdot B = 0 \quad \text{in } \omega^k$$
$$B \cdot n = 0 \quad \text{on } \Gamma^k$$

$Z^k = (Z^{i,k})_{1 \le i \le n}$ is the vector field which gives the direction of the displacement at each node of Γ^k. The vectors $Z^{i,k} \in \mathbb{R}^3$ are associated with the displacements $Z^{i,k}$ which are piecewise linear and related to each knot ξ_i by the formula:

(4.4)
$$Z^{i,k}(x) = \begin{cases} Z^{i,k} N_j(\xi, \eta) & \text{if } x \in T_\ell \text{ and } \xi^i = x^{\ell,j} \in T_\ell \\ 0 & \text{otherwise.} \end{cases}$$

At each iteration, a new surface Γ^{k+1} is constructed from Γ^k by (see [6] for a similar approach):

$$(4.5) \qquad \Gamma^{k+1}(u) = \left\{ X = x + \sum_{i=0}^{n} u_i \, Z^{i,k}(x), u_i \in \mathbb{R}, x \in \Gamma^k \right\}.$$

Then, to update the admissible surface Γ^{k+1} we compute $u = (u_1, \ldots, u_n) \in \mathbb{R}^n$. Moreover, the natural energy associated with $\Gamma^k(u)$ is:

$$(4.6) \qquad E^k(u) = \frac{-1}{2\mu_0} \int_{\omega^k(u)} \|B_u\|^2 \, dy + \sigma \int_{\Gamma^k(u)} d\gamma + \rho g \int_{\Omega^k(u)} x_3 \, dy$$

where $\Omega^k(u)$, $\omega^k(u)$ are respectively the inside and the outside of $\Gamma^k(u)$ and B_u is the solution of (4.3) where $\omega^k(u)$ replaces ω^k. Here the gravity term is given by $G(x) = \rho g x_3$. In fact, B_u^k is a numerical approximation of B_u.

We take into account the constraint on the volume of $\Omega^k(u)$ by a penalty method. Then the penalized energy is the following:

$$(4.7) \qquad E_r^k(u) = E^k(u) + \frac{r}{2}(V(u) - V_0)^2$$

with $V(u)$ the volume of $\Omega^k(u)$ and V_0 given.

A critical point of this penalized energy is computed by a quasi-Newton B.F.G.S. optimization technique [7, 8, 15, 22, 24]. At each iteration we must compute the gradient with respect to u of the energy at $u = 0$. We denote this gradient by $DE_r^k = (D_i E_r^k)_{i=1,\ldots,n}$. The derivatives $D_i E_r^k$ are given by the following lemma which is a discrete version of Lemma 3.1.

Lemma 4.1. *For $i = 1, \ldots, n$ we have:*

$$(4.8) \quad D_i E_r^k = \sum_{\{\ell, T_\ell \ni \xi_i\}} \frac{1}{2\mu_0} \int_{T_r} \|B\|^2 (Z^{i,k} \cdot n) \|x_\xi^\ell \wedge x_\eta^\ell\| \, d\xi \, d\eta$$

$$+ \rho g \int_{T_r} x_3^\ell (Z^{i,k} \cdot n) \|x_\xi^\ell \wedge x_\eta^\ell\| \, d\xi \, d\eta + \sigma \int_{T_r} (\|x_\xi^\ell\|^2 \|x_\eta^\ell\|^2 - (x_\xi^\ell \cdot x_\eta^\ell)^2)^{-1/2}$$

$$\cdot ((x_\xi^\ell \cdot Z_\xi^{i,k}) \|x_\eta^\ell\|^2 + (x_\eta^\ell \cdot Z_\eta^{i,k}) \|x_\xi^\ell\|^2 - x_\xi^\ell \cdot x_\eta^\ell (x_\eta^\ell \cdot Z_\xi^{i,k} + x_\xi^\ell \cdot Z_\eta^{i,k})) \, d\xi \, d\eta$$

$$+ r(V_k - V_0) \int_{T_r} (Z^{i,k} \cdot n) \|x_\xi^\ell \wedge x_\eta^\ell\| \, d\xi \, d\eta$$

where T_r is the reference triangle (coordinates ξ and η), B the solution of problem (4.3), $x^\ell = x(\xi, \eta)$ an arbitrary point of T_ℓ (parametrized by (4.1)), x_ξ^ℓ, x_η^ℓ the vector derivatives of x^ℓ w.r. to ξ and η, $Z_\xi^{i,k}$, $Z_\eta^{i,k}$ the vector derivatives of $Z^{i,k}$ w.r. to ξ and η, V_k the volume of Ω^k (inside of Γ^k).

All these integrals are calculated exactly except the first one; to compute this integral one must know the value of the magnetic vector field B. This imply the resolution of the exterior problem (4.3). This is the most time consuming step of the algorithm.

5. Computation of an approximation of $\|B\|^2$ over Γ^k

The computation of the gradient DE_r^k requires the values of B^k solution of:

$$\nabla \wedge B^k = \mu_0 j_0 \qquad \text{in } \omega^k$$
$$\nabla \cdot B^k = 0 \qquad \text{in } \omega^k$$
$$B^k \cdot n = 0 \qquad \text{on } \Gamma^k.$$

We write $B^k = B_1 + B_2^k$ with B_1 given by (2.5) so that $B_2^k = B^k - B_1$ is solution of:

(5.1)
$$\nabla \wedge B_2^k = 0 \qquad \text{in } \omega^k$$
$$\nabla \cdot B_2^k = 0 \qquad \text{in } \omega^k$$
$$B_2^k \cdot n = -B_1 \cdot n \qquad \text{on } \Gamma^k.$$

As explained in Sect. 2, we have $B_2^k(x) = \nabla_x \varphi^k(x)$ where φ^k is the scalar potential solution of the following Neumann exterior problem:

(5.2)
$$\Delta \varphi^k = 0 \qquad \text{in } \omega^k$$
$$\frac{\partial \varphi^k}{\partial n} = -B_1 \cdot n \qquad \text{on } \Gamma^k$$

$$\varphi^k(x) = O(\|x\|^{-1}), \qquad \|\nabla_x \varphi^k(x)\| = O(\|x\|^{-2}) \text{ as } \|x\| \to \infty.$$

As we need to evaluate $\nabla_x \varphi^k(x)$ only on Γ^k, we choose an integral representation of the solution [6, 23, 30]:

(5.3)
$$\varphi^k(x) = \frac{1}{4\pi} \int_{\Gamma^k} q(y) \frac{1}{\|x - y\|} d\gamma(y)$$

where q is the solution of the following boundary integral equation over Γ^k (see (2.17), (2.18)):

(5.4)
$$B_1(x) \cdot n = \frac{q(x)}{2} + \frac{1}{4\pi} \int_{\Gamma^k} q(y) \frac{n_x \cdot (x - y)}{\|x - y\|^3} d\gamma(y).$$

To solve this second kind Fredholm integral equation, we use a Galerkin method [6, 19, 23]. We introduce a basis $\{e_j^k\}_{j=1,\dots,L}$ where e_j^k is piecewise constant over Γ^k, that is:

$$e_j^k(x) = \begin{cases} 1 & \text{if } x \in T_j \ \forall j = 1, \dots, L (L: \text{the number of triangles over } \Gamma^k) \\ 0 & \text{otherwise} \end{cases}$$

Then the solution q of (5.4) is now approximated by:

$$q^k(y) = \sum_{j=1}^{L} c_j^k e_j^k$$

where $(c_j^k)_{j=1,\dots,L} \in \mathbb{R}^L$ is solution of the following linear system [6, 19]:

(5.6) $(D^k + H^k) \vec{c}^k = \ell^k; \vec{c}^k = (c_j^k)_{j=1,\dots,L}$

(5.7) $D^k = (d_{i,j})_{i,j=1}^L$ and $H^k = (h_{i,j}^k)_{i,j=1}^L$

where

(5.8)
$$h_{i,j}^k = \frac{1}{2\pi} \int_{T_i} \int_{T_j} \frac{n \cdot (x - y)}{\|x - y\|^3} d\gamma(x) d\gamma(y)$$

$$d_{i,j}^k = \begin{cases} 0 & \text{if } i \neq j \\ \int_{T_i} d\gamma(x) & \text{if } i = j \end{cases}$$

(5.9)
$$\ell_i^k = 2 \int_{T_i} B_1(x) \cdot n_i d\gamma(x).$$

The matrix of the system is full and not symmetric. The coefficients h_{ii}^k are equal to zero as $n_i \cdot (x - y) = 0$. Then we can compute $h_{i,j}^k$ by a Newton-Cotes method. Computation of the coefficient ℓ_i strongly depends on $B_1(x)$. It requires numerical quadrature of the expression (2.5).

Finally, computing $\|B^k(x)\|^2 = \|B_1(x) + \nabla_x \varphi^k(x)\|^2$ implies the evaluation of $\nabla_x \varphi^k(x)$ which is given by:

$$(5.10) \qquad \nabla_x \varphi^k(x) = \frac{1}{4\pi} \int_{\Gamma^k} q^k(y) \, \nabla_x \left(\frac{1}{\|x-y\|}\right) d\gamma(y).$$

This is clearly a singular integral as the kernel is $\nabla_x \left(\dfrac{1}{\|x-y\|}\right)$ which has a singularity of order 2. As q^k is a constant on each triangle T_j, this integral is a linear combinatin of elementary integrals like:

$$\int_{T_j} \nabla_x \left(\frac{1}{\|x-y\|}\right) d\gamma(y)$$

which are computed at the barycenter of each triangle T_i. Only the integral where $T_j = T_i$ is singular. Integrating by parts reduces the problem to a simple integral over ∂T_j.

6. Numerical results

We write the energy (1.5) as:

$$(6.1) \qquad E(\Omega) = B_m \int_\omega \|B\|^2 \, d\Omega + \sigma \int_\Gamma d\Gamma + B_g \int_\Omega z \, d\Omega$$

where the constants B_m, σ and B_g are given various values.

6.a. Some extra information on the actual computation

We slightly modify the algorithm described in Sect. 4 in order to improve the efficiency and reduce the computing time.

For instance, we start with a coarse grid to obtain a first rough approximation of the free surface. Once the coarse approximation in calculated, we use a refinement technique to work on a finer mesh. The displacement direction vector field Z_i associated with each knot ξ_i is modified at each iteration. New directions are obtained using the normalized average of the normal vectors to the triangles in the neighbourhood of the ξ_i node. The linear systems are solved by a minimal residual algorithm.

The code was vectorized for a CRAY II computer. Indeed, in the boundary integral representation method, one of the most costly parts is the evaluation of the coefficients of the linear system matrix (5.6). In this section of the algorithm, we compute $h_{i,j}^k$ (see (5.8)), that is to say a double integral over each pair of triangles T_i, T_j. The vectorisation of this part of the algorithm provided a significant improvement and reduced the global time by five. The C.P.U. time for a gradient evaluation in a CRAY II computer in a case of 480 finite elements is about two seconds.

We do not have much control on the number of iterations since we do not really use any one-dimensional optimization strategy to optimize the line search in the quasi-Newton method. Indeed this would require lengthly evaluations of the magnetic field far from the free surface. We chose to allow more iterations. More analysis is now being made to improve this point.

6.b. The examples

We now present six different examples; in all cases we start with a sphere and a mesh of 480 finite elements.

In Fig. 1 we present two views of a bubble where the magnetic field B is created by three wires with a symmetric configuration. We do not take into account the potential energy due to the gravity as $B_g = 0$. Numerical convergence is obtained after 168 gradient evaluations (see remark above) and the final number of finite elements is 736.
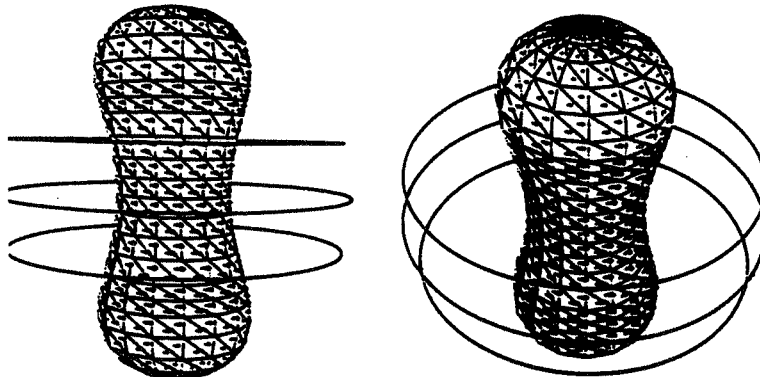

Fig. 1. $-B_m = 1$; $B_g = 0$; $\sigma = 0.1$; kel $= 736$ and icount $= 168$

In Fig. 2 the magnetic field B is created by seven wires, the configuration is also symmetric. Here we take into account the gravity since $B_g = 0.1$. Numerical convergence is obtained after 186 gradient evaluations and the number of finite elements is 576.
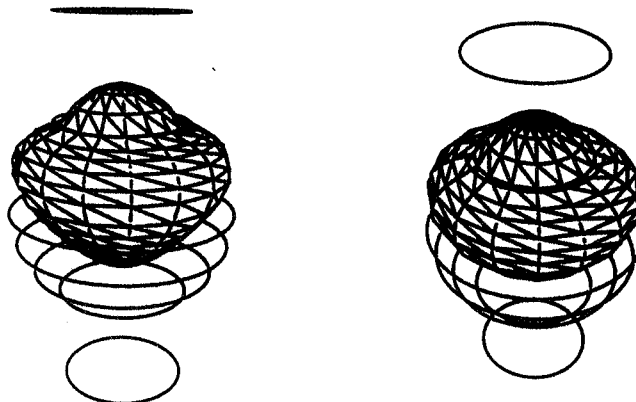

Fig. 2. $-B_m = 1$; $B_g = 0.1$; $\sigma = 1$; kel $= 576$ and icount $= 186$

In Fig. 3 the magnetic field *B* is created by seven wires, but now the configuration is not symmetric. The free surface obtained is clearly not symmetric either. Here we take into account the gravity since $B_g = 0.1$. Numerical convergence is obtained after 208 gradient evaluations and the number of finite elements is 576.
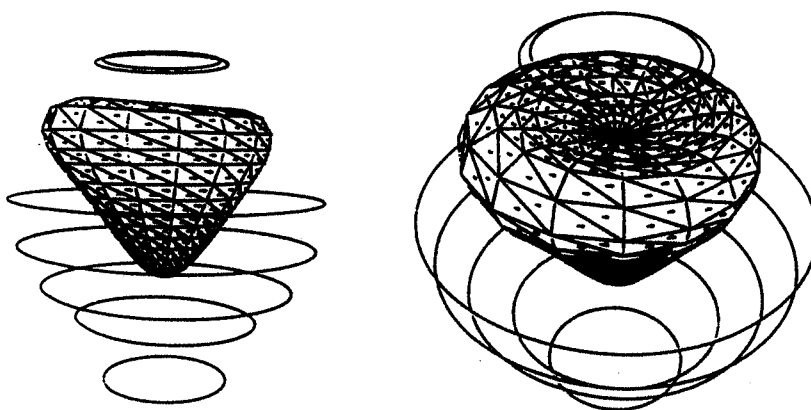

Fig. 3. $-B_m = 1.0$; $B_g = 0.1$; $\sigma = 0.1$; kel = 576 and icount = 208

In Fig. 4 the magnetic field *B* is created by the same seven wires as in the previous example but here the sense of the current has been changed in the two wires on the top. Numerical convergence is obtained after icount = 156 evaluations of the gradient and the number of finite elements kel is 608.
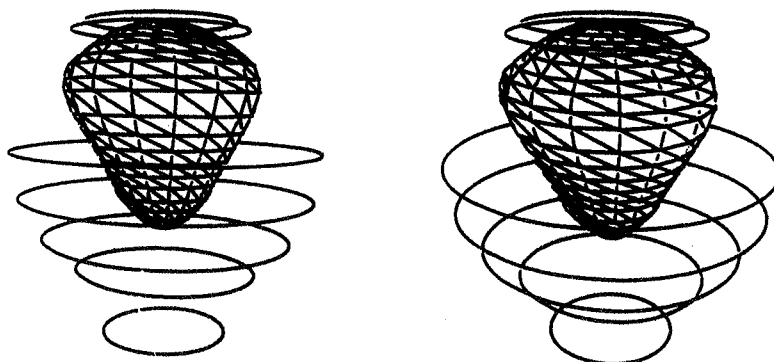

Fig. 4. $-B_m = 1.0$; $B_g = 0.1$; $\sigma = 0.1$; kel = 608 and icount = 156

In Fig. 5 the magnetic field B is created by only one wire which turns around the liquid metal bubble. The factor of the energy due to the magnetic field B_m is 50. Numerical convergence is obtained after 248 evaluations of the gradient and with 544 finite elements.
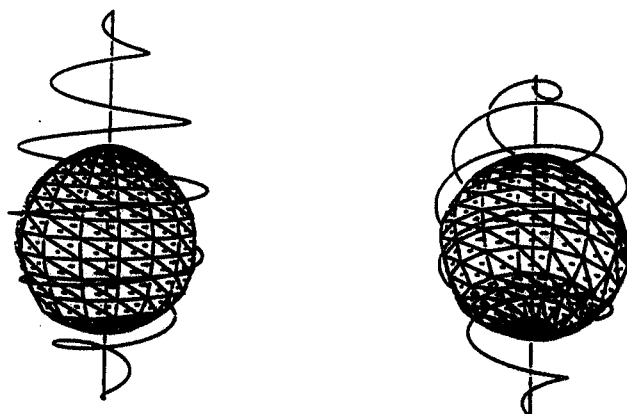

Fig. 5. $-B_m = 50.0$; $B_g = 0.1$; $\sigma = 0.1$; kel $= 544$ and icount $= 248$

In Fig. 6 we present the same example as before but now B_m is 100. We observe that the position of the liquid metal bubble is not the same. Convergence is obtained in 240 evaluations of the gradient and with 480 finite elements.
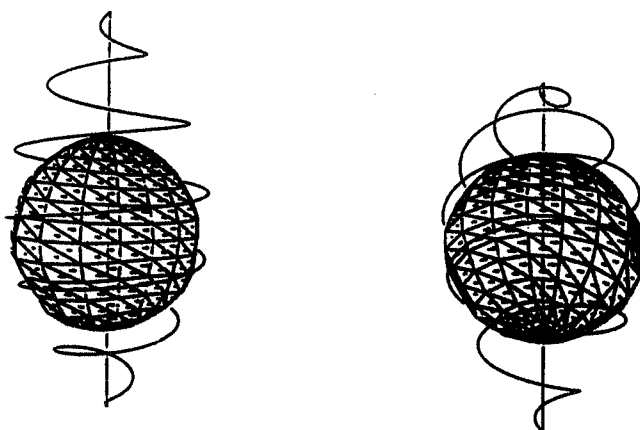

Fig. 6. $-B_m = 100.0$; $B_g = 0.1$; $\sigma = 0.1$; kel $= 480$ and icount $= 240$

References

1. Atkinson, K.E. (1990): A survey of boundary integral equations methods for the numerical solution of Laplace's equation in three dimensions. In: M.A. Golberg ed., Math. Concepts Methods Sci. Eng. 42, pp. 1–34 Plenum Press

2. Brancher, J.-P., Etay, J., Sero-Guillaume, O. (1983): Formage d'une lame. J. de Mécanique Théorique et Appliquée. **2** (6) 976–989

3. Brancher, J.-P., Sero-Guillaume, O. (1983): Sur l'équilibre des liquides magnétiques, applications à la magnétostatique. J. de Mécanique Théorique et Appliquée. **2** (2) 265–283

4. Coulaud, O., Henrot, A. (1991): A nonlinear boundary value problem solved by spectral methods. Appl. Anal. **43**, 229–244

5. Coulaud, O., Henrot, A. (1993): Numerical approximation of a free boundary problem arising in electromagnetic shaping 237–303 (to appear)

6. Dautray, R., Lions, J.-L. (1988): Analyse mathématique et calcul numérique pour les Sciences et les Techniques. **5** (6)

7. Dennis J.E., JR., More, J.J. (1977): Quasi-Newton method motivation and theory. SIAM Review **19** (1) 46–89

8. Dennis J.E., JR., Schnabel, R.B. (1983): Numerical methods for unconstrained optimization and nonlinear equations. Prentice-Hall, Englewood Cliffs, NJ

9. Descloux, J. (1990): On the two dimensional magnetic shaping problem without surface tension. Report n° 07.90, Ecole Polytechnique Fédérale de Lausanne, Suisse

10. Etay, J. (1982): Le formage électromagnétique des métaux liquides. Aspects expérimentaux et théoriques. Thèse Docteur-Ingénieur. U.S.M.G., I.N.P.G. Grenoble, France

11. Etay, J., Mestel, A.J., Moffatt, H.K. (1988): Deflection of a stream of liquid metal by means of an alternating magnetic field. J. Fluid Mech. **194**, 309–331

12. Gagnoud, A., Brancher, J.-P. (1985): Proceedings of the Conference of Computation of Electromagnetic Fields. Fort Collins, USA

13. Gagnoud, A., Etay, J., Garnier, M. (1986): Le problème de frontière libre en lévitation électromagnétique. J. de Mécanique Théorique et Appliquée, **5** (6) 911–925

14. Gagnoud, A., Sero-Guillaume, O. (1986): Le creuset froid de lévitation: modélisation électromagnétique et application. E.D.F. Bull. Etudes et Recherches, Série B, **1**, 41–51

15. Gilbert, J.-Ch., Lemarechal, C. (1988): Some numerical experiments with variable storage Quasi-Newton algorithms. IIASA Working Paper WP, **88** (121) p. 2361. Laxenburg, Austria

16. Grisvard, P. (1985): Elliptic problems in non smooth domains. Monogr. Stud. Math. **24**

17. Henrot, A., Pierre, M. (1989): Un problème inverse en formage de métaux liquides. M^{2}AN, **23**, 155–177

18. Hornung, U., Mittelmann, H.D. (1988): The augmented skeleton method for parametrized surfaces of liquid drops. Technical Report N°113. Arizona State University, Tempe, AZ

19. Johnson, C.G.L., Scott, L.R. (1989): An analysis of quadrature errors in second-kind boundary integral methods. Siam J. Numer. Anal. **26** (6) 1356–1382

20. Li, B.Q., Evans, J.W. (1989): Computation of shapes of electromagnetically supported menisci in electromagnetic casters. Part. I: Calculations in the two dimensions. IEEE Trans. Magnetics. **25** (6) 4442

21. Mestel, A.J. (1982): Magnetic levitation of liquid metals. J. Fluid Mech. **117**, 27–43

22. Minoux, M. (1983): Programmation mathématique; théorie et algorithmes, tome 1. Dunod, Paris

23. Nédelec, J.C. (1977): Approximation des équations intégrales en mécanique et en physique. Rapport, Centre de Mathématiques Appliquées, Ecole Polytechnique, Palaiseau, France

24. Oren, S.S., Spedicato, E. (1976): Optimal conditioning of self-scaling variable metric algorithms. Math. Program. **10**, 70–90

25. Pierre, M., Roche, J.-R. (1991): Numerical computation of free boundaries in 2-d electromagnetic shaping. Eur. J. Mech., B**10** (5) 489–500

26. Sero-Guillaume, O. (1983): Sur l'équilibre des ferrofluides et des métaux liquides. Thèse, Institut Polytechnique de Lorraine, Nancy, France

27. Simon, J. (1988): Second variations for domain optimization problems. Control of distributed parameter systems. Proceedings 4th International Conference in Vorau, Birkhauser, Basel

28. Sneyd, A.D., Moffatt, H.K. (1982): Fluid dynamical aspects of the levitation melting process. J. of Fluid Mech. **117**, 45–70

29. Zolésio, J.P. (1981): The Material derivative (or speed) method for shape optimization. In: J. Cea, E.J. Hand, eds., Optimization of Distributed Parameter Structures vol. II. pp. 1089–1151. Sijhoff and Nordhoff, Alphen aan den Rijn
30. Zolésio, J.P. (1984): Numerical algorithm and existence result for a Bernoulli-like problem steady free boundary problem. Large Scale Syst. 6 (3) 263–278
31. Zolésio, J.P. (1990): Introduction to shape optimisation problems and free boundary problems. Séminaire de Mathématiques Supérieures. Université de Montréal, Montréal, Canada